



Original Article

Monte Carlo simulations of chromium target under proton irradiation of 17.9, 22.3 MeV

A. Kara^{a,*}, A. Yılmaz^a, M. Yiğit^b^a Department of Electrical and Electronics Engineering, Giresun University, 28200, Giresun, Turkey^b Department of Physics, Aksaray University, 68100, Aksaray, Turkey

ARTICLE INFO

Article history:

Received 10 November 2020

Received in revised form

21 April 2021

Accepted 27 April 2021

Available online 17 May 2021

Keywords:

Chromium
Radiation damage
TALYS
SRIM
GEANT4

ABSTRACT

Chromium material is commonly used for fusion plasma facing applications because of the low neutron activation property. The Monte Carlo method is one of the useful ways to investigate the ion-target interactions. In this study, Chromium target irradiated by protons was investigated using Monte Carlo based simulation tools. In this context, the calculations of radiation damage on Chromium material irradiated with protons at 17.9 and 22.3 MeV energies were carried out using GEANT4 and SRIM codes. Besides, the cross sections for proton interaction with Chromium target were calculated by the TALYS 1.9 code using CTM + FGM, BSFGM, and GSFM level densities. As a result, GEANT4, SRIM and TALYS 1.9 codes provide a suitable tool for the predictions of radiation damage and cross cross section with proton irradiation.

© 2021 Korean Nuclear Society, Published by Elsevier Korea LLC. This is an open access article under the CC BY-NC-ND license (<http://creativecommons.org/licenses/by-nc-nd/4.0/>).

1. Introduction

Global energy demand is growing rapidly, because of population and economic growth. In this context, if nuclear fusion energy can be commercialized, it can be a hope for humanity and the future of the world. However, the reliable functioning and structural integrity of fusion reactors depend on experiments and calculations containing the interactions of charged particles with structural fusion materials. These experiments lead to material burden and a huge waste of time. Therefore, the nuclear model calculations are great contributions before the engineering applications [1–5]. Choice of the material against high-temperature and nuclear radiation provides an important contribution to the success of the reactor [3,6]. As with fission reactors, the use of steel in the design of fusion reactors is quite common. Cr material is the most versatile and widely used element in steel alloying. It is commonly used in fusion plasma-facing applications due to the low neutron activation property. In this study, the calculations on the cross section and detailed radiation damage for Chromium irradiated with protons at 17.9 and 22.3 MeV energies are performed using GEANT4 [7,8], SRIM [9,10] and TALYS 1.9 [11] codes based on Monte Carlo methods.

2. Monte Carlo simulations

The consistent calculation and analysis using nuclear models are the requirement to explain the particle-target nucleus interactions. The further improvement of nuclear structure and reaction theory depends on which linked to put forward new nuclear models and to figure out nucleoninduced reactions [4,12–16]. TALYS is software that is widely used and allows us to examine the mechanisms of nuclear reaction in detail. It is known that it provides success in the simulation of particle and photon-induced nuclear reactions especially in the range of 1 keV and 200 MeV energy. The TALYS code provides

a complete description of all reaction channels and observables and is also user-friendly. Besides, this code also provides information to the user about the energy spectrum, distribution, and even angle-related situations. Obtaining the nuclear cross section calculations in the code uses various microscopic and phenomenological level density models. Besides, the TALYS code allows us to study the direct interaction, equilibrium, and pre-equilibrium processes in detail Koning et al. [11]. The calculations of the equilibrium and pre-equilibrium emissions at this code can be made by the Hauser-Feshbach model [17] and Exciton model [18]; respectively. TALYS reaction code uses the optical model parameterization for protons and neutrons on a nucleus-by-nucleus basis for obtaining the nuclear cross sections and the transition coefficients.

* Corresponding author.

E-mail address: ayhankara@gmail.com (A. Kara).

The spectrum of the pre-equilibrium particle emission in the TALYS reaction code is given as,

$$\frac{d\sigma_k^{PE}}{dE_k} = \sigma^{CF} \sum_{p_\pi=p_\pi^0}^{p_\pi^{\max}} \sum_{p_\nu=p_\nu^0}^{p_\nu^{\max}} W_k(p_\pi, h_\pi, p_\nu, h_\nu, E_k) \tau(p_\pi, h_\pi, p_\nu, h_\nu) \times P(p_\pi, h_\pi, p_\nu, h_\nu) \quad (1)$$

where, the $h_\pi(h_\nu)$ and $p_\pi(p_\nu)$ are the proton (neutron) hole number and the proton (neutron) particle number, respectively. E_k and W_k correspond to the emission energy and emission rate for an ejectile k , respectively. σ^{CF} represents the compound-nucleus formation cross section predicted using the optical model. P denotes the part of the pre-compound flux for the emission to survive the previous states and now passes through the $(p_\pi, h_\pi, p_\nu, h_\nu)$ configurations, averaged over time. The quantity τ is the average lifetime of the exciton state. The initial neutron and proton particle numbers correspond to the terms $p_\nu^0 = N_p$ and $p_\pi^0 = Z_p$, respectively with $Z_p(N_p)$ the proton (neutron) number of the incident particle [11]. The total level density can be written as,

$$\rho^{tot}(E_x) = \sum_J \sum_\Pi \rho(E_x, J, \Pi) \quad (2)$$

where the level density $\rho(E_x, J, \Pi)$ at a certain spin J and parity Π is the number of levels per MeV around E_x excitation energy [11].

SRIM (The Stopping and Range of Ions in Matter), a widely used tool for binary collision approximation simulations, uses semi-empirical relations. The SRIM code founded by Ziegler is software that examines the effects of ion and atom interactions with a quantum mechanical approach [9]. It uses the Bethe-Bloch expression to calculate stopping power. This code has many applications such as sputtering ion, transmission, ion's energy loss, target damage, ion stopping in targets, ion implantation, and ion beam therapy [9,10].

GEANT4 (GEometry ANd Tracking) is a simulation toolkit written in C++ language, which permits us to make a detailed simulation of the propagation of particles interacting with materials [7,8]. This code has widespread use including the simulation of the

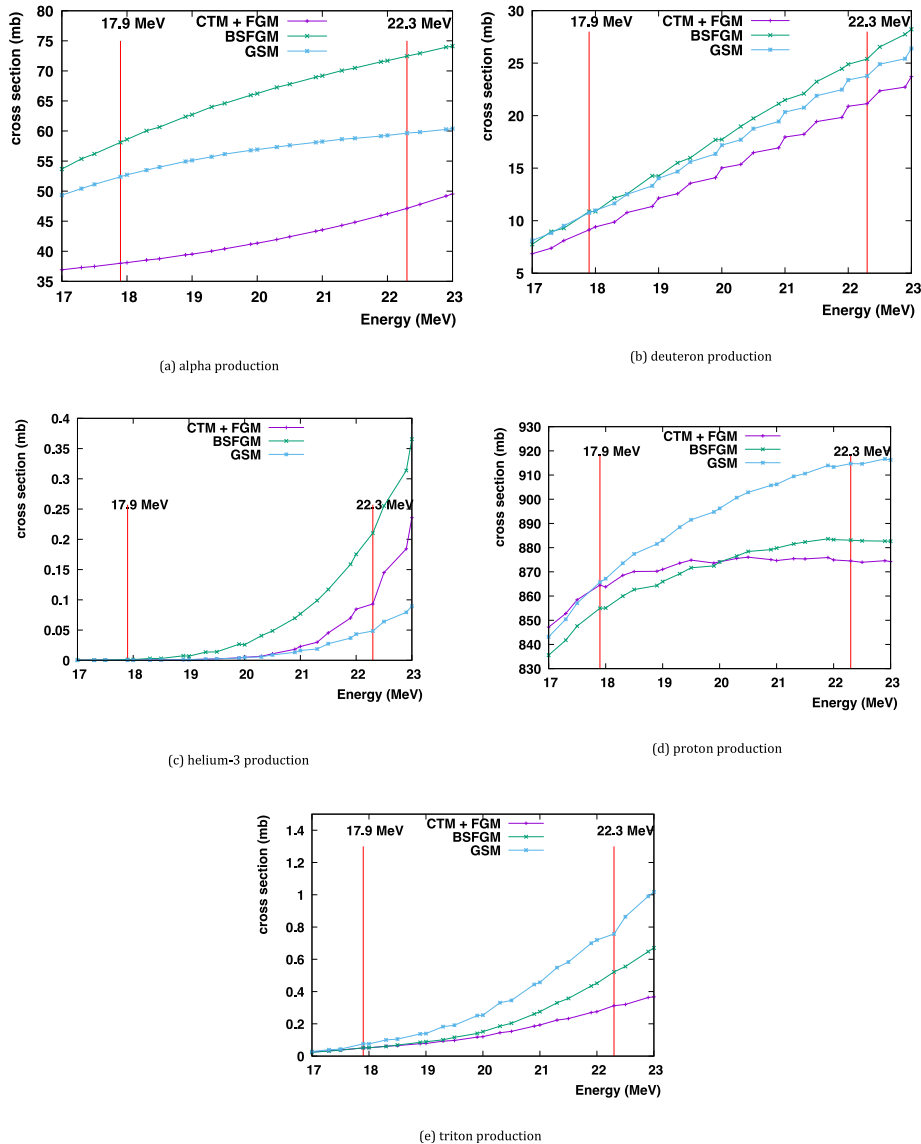


Fig. 1. Total cross section of particle production in $p + {}^{nat}\text{Cr} \rightarrow X$ reaction using the TALYS 1.9 simulation program.

model and experimental data ranging from medical and nuclear physics to high-energy astrophysics, as well as of course accelerator design and particle physics. Geant4 includes a comprehensive set of physics processes modeling the behavior of particles. The design of the Geant4 visualization is generated to visualize tracking steps, detector geometry, particle trajectories, texts (character strings), hits, etc., to help users to execute and prepare a realistic detector simulation [7].

Table 1
The calculation results for particle production cross sections at 17.9 and 22.3 MeV.

Model calculations	Energy (MeV)	Cross Section (mb)				
		Alpha	Deuteron	Helium-3	Proton	Triton
CTM + FGM	17.9	38.01	9.12	0.00034	864.53	0.049
	22.3	47.12	21.13	0.093	874.49	0.31
BSFGM	17.9	58.11	10.86	0.0013	854.95	0.051
	22.3	72.45	25.39	0.21	883.09	0.52
GSM	17.9	52.38	10.75	0.00031	865.73	0.076
	22.3	59.65	23.76	0.048	914.70	0.75

3. Results and discussion

The choice of material for the reactor and the detection of events as a result of a reaction are of great importance for the sustainability of the reactor. Lightweight particles, which are known as Helium-3, proton, neutron, alpha, triton, deuteron, formed as a result of a nuclear reaction during an irradiation process, can be accumulated as gas in the material and this accumulation can lead to nuclear damage. In the present study, gas production cross sections for chromium irradiated with protons at 17.9 and 22.3 MeV energies were calculated by using the Constant Temperature model + Fermi Gas model (CTM + FGM) [19]; the Back-shifted Fermi Gas model (BS-FGM) [20] and the Generalized Superfluid model (GSFM) [21] in TALYS code, and were presented in Fig. 1. Furthermore, the calculated data are given numerically in Table 1. Level density models have a key role in accurately predicting nuclear cross sections [22–28].

It is clear from Fig. 1 that the cross sections vary significantly depending on the energy of the incident particle. Although this seems to be an expected situation, the values obtained after certain energy have seemed with different scenarios, such as decreasing or

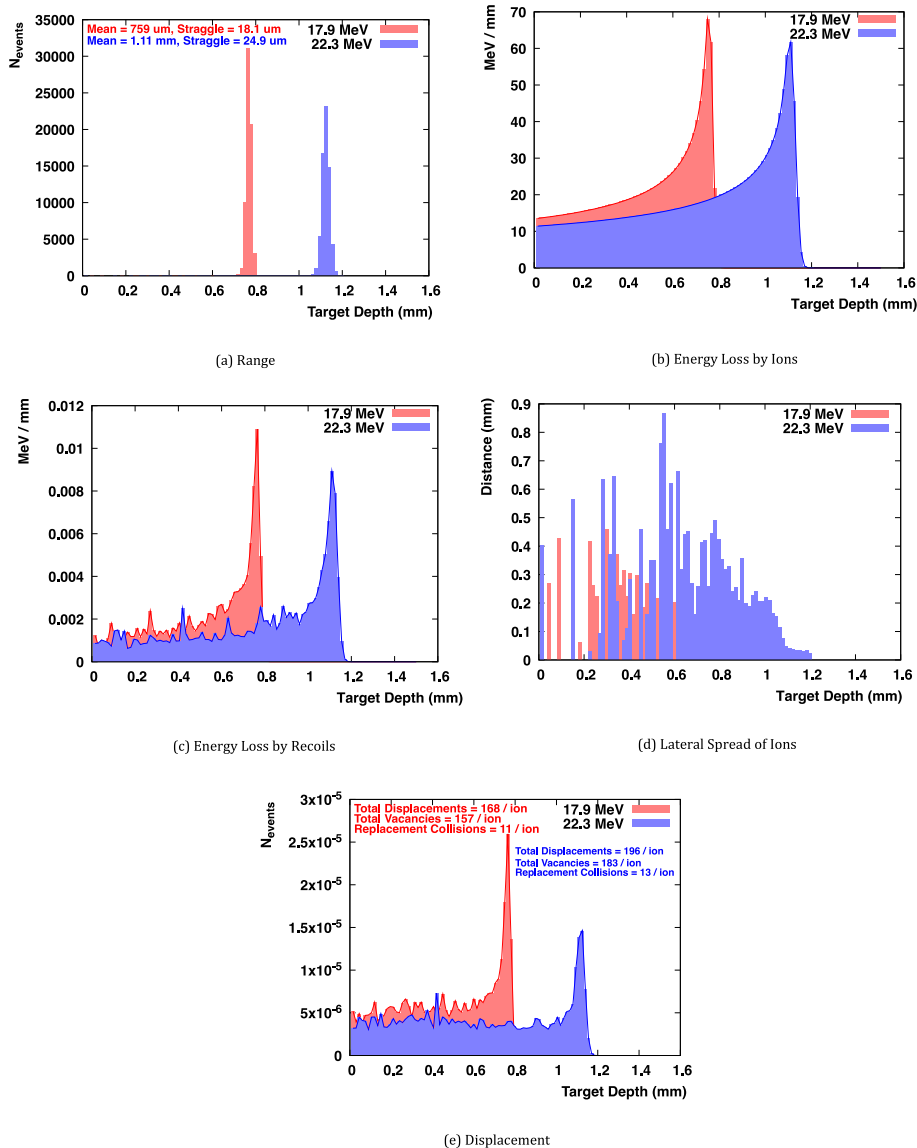


Fig. 2. The calculation results by SRIM code for H ions in Cr target of 17.9 and 22.3 MeV. (a) the projected range of H ions in the Cr target, (b) the ionization energy loss, (c) the recoil energy loss, (d) the lateral spread of the ions, (e) the total displacements.

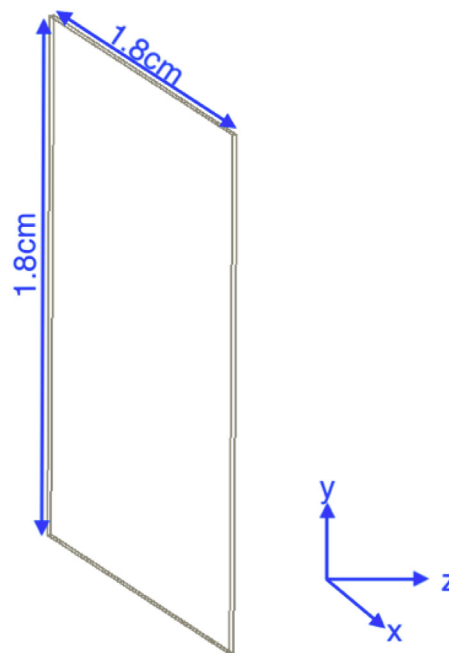
increasing tendency. It is evident from Table 1 that the noticeable difference between the calculations on different level density models is observed for alpha production cross sections. In addition, the cross section values of proton production are significantly higher than other particles. As seen in Fig. 1c, there is almost no Helium-3 production up to 18 MeV. The agreement between the different level density models of cross section results for the irradiation with 17.9 MeV protons is satisfactory except for alpha production. On the other hand, there is more difference between the results obtained for the protons at energies of 22.3 MeV.

The calculations on stopping power of target material for charged particles are very useful in understanding the interaction of particles with matter. The interaction of Chromium target irradiated with protons were calculated using SRIM code and the obtained results are shown in Fig. 2. Stopping power and penetrating distances for this interaction are also given numerically in Table 2. The stopping power in chromium target decreases with increasing the proton energy. It is clear from that the interactions occurring inside the Cr targets irradiated by protons strongly depend on ion penetration range. In addition, the electronic stopping for protons in Cr target is about a factor of 1000 bigger than the nuclear stopping.

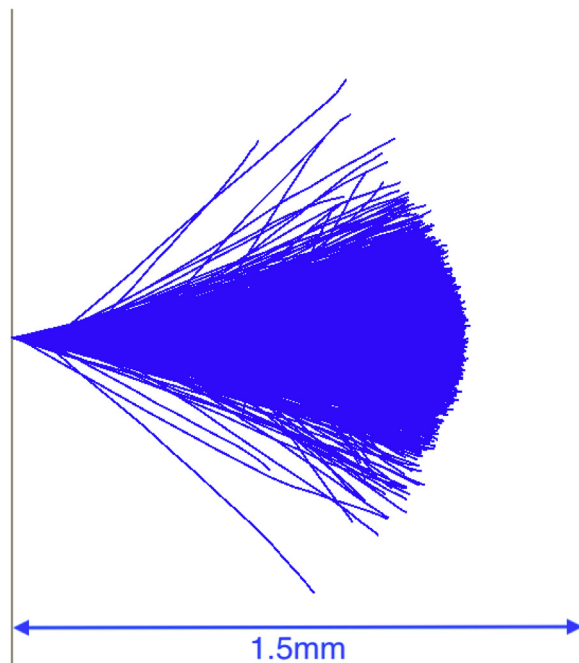
Table 2
Stopping parameters for protons in Cr target up to 30 MeV energy.

Proton Energy (MeV)	Stopping power (Electronic) (MeV cm ² /mg)	Stopping power (Nuclear) (MeV cm ² /mg)	Projected Range (μm)
0.5	200.8	0.1832	2.57
0.7	167.7	0.1391	4.07
1	137.1	0.1035	6.79
1.2	123.0	0.0886	8.91
1.5	107.4	0.0736	12.50
1.7	99.31	0.0662	15.16
2	89.57	0.0576	19.53
2.25	83.00	0.0521	23.52
2.5	77.45	0.0476	27.81
2.75	72.71	0.0439	32.39
3	68.59	0.0407	37.26
3.25	64.97	0.0380	42.41
3.5	61.77	0.0357	47.84
3.75	58.91	0.0336	53.55
4	56.34	0.0318	59.52
4.5	51.89	0.0287	72.25
5	48.18	0.0262	86.02
5.5	45.02	0.0241	100.81
6	42.30	0.0223	116.60
6.5	39.92	0.0208	133.36
7	37.83	0.0195	151.09
8	34.31	0.0173	189.35
9	31.46	0.0156	231.31
10	29.09	0.0142	276.89
11	27.09	0.0131	326.01
12	25.37	0.0121	378.61
13	23.89	0.0113	434.62
14	22.59	0.0106	494.00
15	21.43	0.0099	556.69
16	20.41	0.0094	622.65
17	19.48	0.0089	691.83
18	18.65	0.0084	764.19
20	17.20	0.0077	918.25
21	16.61	0.0074	999.86
22	16.01	0.0071	1008
22.5	15.72	0.0069	1130
25	14.49	0.0063	1360
27.5	13.47	0.0058	1600
30	12.59	0.0053	1870

We simulated for 100000 ions impinging on Chromium target at 17.9 MeV and 22.3 MeV beam energy.



(a)



(b)

Fig. 3. Simulated target geometry in GEANT4 program and generated particle shower inside the target medium.

Fig. 2a shows the final ion positions for 17.9 MeV (22.3 MeV) energy. Here, the projected range of ion is 0.759 mm (1.11 mm) and its straggling 0.018 mm (0.024 mm). The dependence of energy losses on the projected range in Cr target which has 1.5 mm thickness is depicted in Fig. 2b for ions and Fig. 2c for recoils. The maximum dE/dx values for ions and recoils reach 68.05 MeV/mm (61.74 MeV/mm) and 0.0109 MeV/mm (0.0089 MeV/mm), respectively. Above the maximum, the energy deposition drops sharply. Fig. 2d shows that the ion Lateral Projected Range (which is defined as the average of the absolute values of the projected lateral displacements from the x-axis) is 0.027 mm (0.039 mm) and its straggling is 0.038 mm (0.055 mm). It can be seen from Fig. 2e that the total displacements, the total vacancies and total replacement collisions for the energy of 17.9 MeV (22.3 MeV) are 168/Ion (196/Ion), 157/Ion (183/Ion) and 11/Ion (13/Ion), respectively. Most of the displacements created by protons at the energy of 17.9 and 22.3 MeV occur in the region of approximately 0.759 mm and 1.11 mm, respectively. GEANT4 (v10.5.0) simulation program provides numerous physics models describing particle interactions. To get higher accuracy of electrons, hadrons, and ion tracking results, emstandard_opt4, is a new physics constructor, and the most

accurate standard and low-energy interaction models were selected, and 100000 particles were taken into account in the simulation.

17.9 MeV and 22.3 MeV mono-energetic proton, in front of a Chromium target slab which has a density of 7.18 g/cm³ and dimension of 1.8 cm × 1.8 cm and 1.5 mm, was constructed in the simulation program shown in Fig. 3.

The depth-dose profiles were integrated along the z-axis. The simulation results calculated using GEANT4 code are presented in Fig. 4. From Fig. 4a, the projected range for protons inside Cr target for 17.9 MeV (22.3 MeV) energy is 0.77 mm (1.13 mm). Results show that all incident particles are absorbed inside the target material, are depicted in Fig. 4a. Fig. 4b depicts that the total energy deposited in target material. Since the target material, Cr is dense and of adequate thickness, 100% of primary protons are absorbed. Fig. 4c presents the dependence of energy losses on the projected range of protons in Cr target. As can be seen in Fig. 4c, the maximum dE/dx value at 17.9 MeV (22.3 MeV) reaches 81.129 MeV/mm (66.068 MeV/mm). The plot of the exclusive energy loss along the trace of a charged particles is known as a Bragg curve. The particular energy loss increases roughly as 1/E as predicted by the

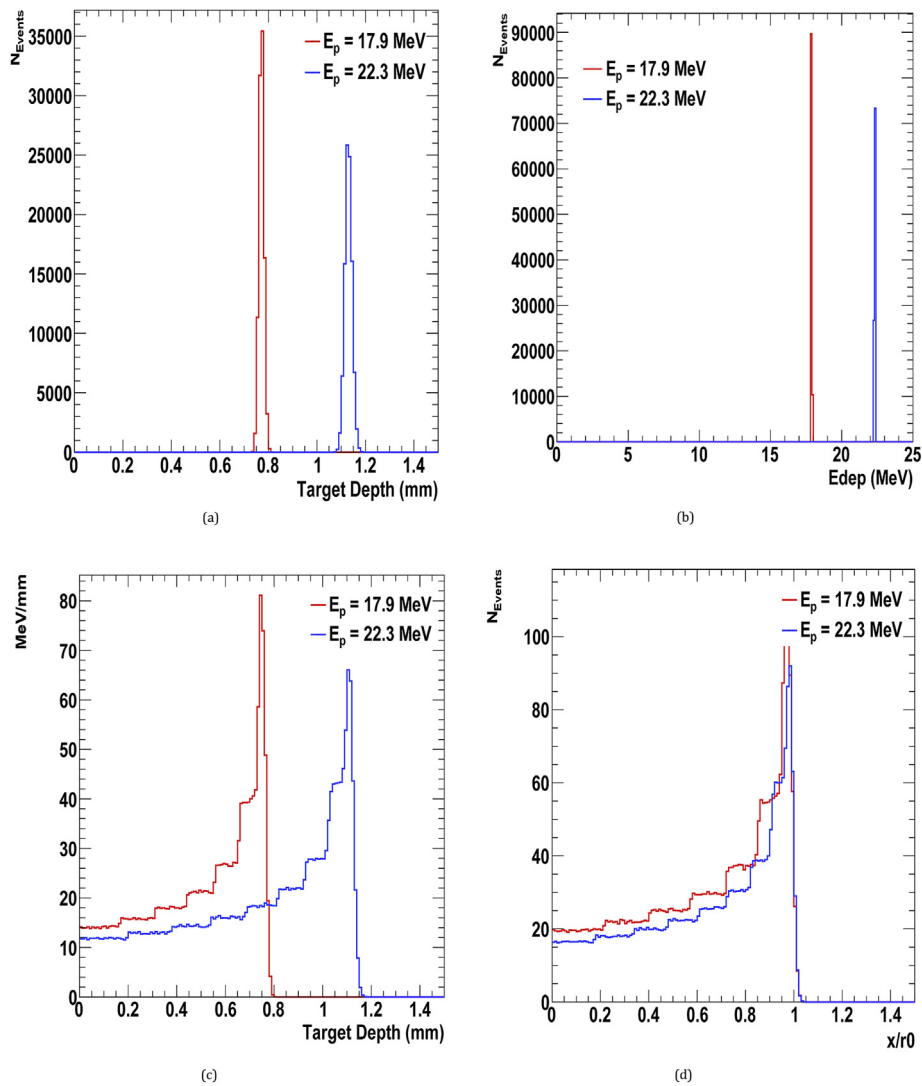


Fig. 4. a) The Number of the particle distribution of initially monoenergetic protons versus penetration distances in Cr target. b) Total number of events versus deposited energy in Cr target for 17.9 MeV and 22.3 MeV primary protons, c) The linear energy transfer for incident protons along with the Cr target material per each event, d) Normalized energy deposition profile inside the Cr target material.

Bethe formula for most of the trace of particles. The charge is lessened due to the electron pickup and the curve diminishes around the end of the track. Fig. 4d shows that longitudinal energy profile as a function of x/r_0 where r_0 is the range of the proton primary particle. Unlike low-energy primary protons, higher energy primary protons leave more energy and penetrate deeper.

4. Conclusion

This study was conducted on chromium material, which is an element well known to the nuclear industry, particularly frequently used in fusion plasma and reactor designs. First of all, a certain thickness value has been chosen for the chromium and then irradiated with the proton at the energy of 17.9 MeV and 22.3 MeV. Because the experimental cross section data at interaction of protons on Cr target are unavailable for the investigated reactions, for this reason, theoretical comparisons were made. It has been observed that the proton production cross section values are higher than other particles for $p + {}^{nat}\text{Cr} \rightarrow X$ reaction, and Helium-3 production was not observed up to almost 18 MeV in all possible situations. According to SRIM code calculations, the electronic energy loss of protons in Cr target is about a factor of 1000 bigger than the nuclear energy loss. It was observed that the maximum dE/dx values obtained by GEANT4 code are 10–15% higher than SRIM calculations. On the other hand, the projected range values of ions in target give very close results for GEANT4 and SRIM codes at 17.9 MeV and 22.3 MeV energies. The results obtained from both are thought to shed light on experimental studies.

Declaration of competing interest

The authors declare that they have no known competing financial interests or personal relationships that could have appeared to influence the work reported in this paper

Acknowledgement

This work was partially supported by the Giresun University Scientific Research Projects Coordination Department under the project Grant no. FEN-BAP-A-250221-49.

References

- [1] M. Yigit, E. Tel, Theoretical determination of (d,n) and (d, 2n) excitation functions of some structural fusion materials irradiated by deuterons, *Nucl. Sci. Tech.* 28 (2017) 165, <https://doi.org/10.1007/s41365-017-0316-6>.
- [2] M. Yigit, Investigating the (p,n) excitation functions on 104–106,108,110pd isotopes, in: *Applied Radiation and Isotopes*, vol. 130, 2017, pp. 109–114, <https://doi.org/10.1016/j.apradiso.2017.09.027>. URL:<http://www.sciencedirect.com/science/article/pii/S0969804317309326>.
- [3] H. Korkut, T. Korkut, A. Kara, M. Yigit, E. Tel, Monte Carlo simulations of 17.9–22.3 mev energetic proton irradiation effects on bcc-zirconium fusionic materials, *J. Fusion Energy* 35 (2016) 591–596, <https://doi.org/10.1007/s10894-016-0068-z>. doi:10.1007/s10894-016-0068-z. URL:..
- [4] M. Yigit, A. Kara, Model-based predictions for nuclear excitation functions of neutron-induced reactions on 64, 66-68 zn targets, *Nucl. Eng. Technol* 49 (2017) 996–1005, <https://doi.org/10.1016/j.net.2017.03.006>. URL:<http://www.sciencedirect.com/science/article/pii/S173857331730061X>.
- [5] M. Yigit, M.E. Korkmaz, On the behavior of cross-sections of charged particle-induced reactions of 181ta target, *Mod. Phys. Lett.* 33 (2018) 1850155, <https://doi.org/10.1142/s0217732318501559>.
- [6] O. Noori-kalkhoran, M. Gei, Evaluation of neutron radiation damage in zircaloy fuel clad of nuclear power plants: a study based on pka and dpa calculations, *Prog. Nucl. Energy* 118 (2020) 103079, <https://doi.org/10.1016/j.pnucene.2019.103079>. URL:<http://www.sciencedirect.com/science/article/pii/S0149197019301805>.
- [7] S. Agostinelli, J. Allison, K. Amako, et al., Geant4—a simulation toolkit, in: *Nuclear Instruments and Methods in Physics Research Section A: Accelerators, Spectrometers, Detectors and Associated Equipment*, vol. 506, 2003, pp. 250–303, [https://doi.org/10.1016/S0168-9002\(03\)01368-8](https://doi.org/10.1016/S0168-9002(03)01368-8). URL:<http://www.sciencedirect.com/science/article/pii/S0168900203013688>.
- [8] J. Allison, K. Amako, J. Apostolakis, et al., Recent developments in geant4, in: *Nuclear Instruments and Methods in Physics Research Section A: Accelerators, Spectrometers, Detectors and Associated Equipment*, vol. 835, 2016, pp. 186–225, <https://doi.org/10.1016/j.nima.2016.06.125>. URL:<http://www.sciencedirect.com/science/article/pii/S016890016306957>.
- [9] J.F. Ziegler, Srim-2003 (Proceedings of the Sixteenth International Conference on Ion Beam Analysis), *Nuclear Instruments And Methods In Physics Research Section B: Beam Interactions With Materials And Atoms*, 219–220, 1027 – 1036, 2004, <https://doi.org/10.1016/j.nimb.2004.01.208>. URL:<http://www.sciencedirect.com/science/article/pii/S0168583X04002587>.
- [10] J.F. Ziegler, M. Ziegler, J. Biersack, Srim – the stopping and range of ions in matter, *Nucl. Instrum. Methods Phys. Res. Sect. B Beam Interact. Mater. Atoms* 268 (2010) 1818–1823, <https://doi.org/10.1016/j.nimb.2010.02.091>. URL: <http://www.sciencedirect.com/science/article/pii/S0168583X10001862>.
- [11] A. Koning, S. Hilaire, S. Goriely, User manual of talys-1.9, URL: <http://talys.eu/download-talys/>, 2017.
- [12] M. Sadeghi, N. Zandi, M. Bakhtiari, Nuclear model calculation for cyclotron production of 61cu as a PET imaging, *J. Radioanal. Nucl. Chem.* 292 (2011) 777–783, <https://doi.org/10.1007/s10967-011-1557-1>.
- [13] L. Mokhtari Oranj, T. Kakavand, M. Sadeghi, M. Aboudzadeh Rovias, Monte Carlo fluka code simulation for study of 68ga production by direct proton-induced reaction, *Nucl. Instrum. Methods Phys. Res. Sect. A Accel. Spectrom. Detect. Assoc. Equip.* 677 (2012) 22–24, <https://doi.org/10.1016/j.nima.2012.02.029>. URL: <https://www.sciencedirect.com/science/article/pii/S0168900212002227>.
- [14] M. Sadeghi, N. Jokar, T. Kakavand, H. Ghafoori Fard, C. Tenreiro, Prediction of 67ga production using the Monte Carlo code mcnpX, *Appl. Radiat. Isot.* 77 (2013) 14–17, <https://doi.org/10.1016/j.apradiso.2013.02.001>. URL: <https://www.sciencedirect.com/science/article/pii/S0969804313000481>.
- [15] L. Deilami-nezhad, L. Moghaddam-Banaem, M. Sadeghi, M. Asgari, Production and purification of scandium-47: a potential radioisotope for cancer theranostics, *Appl. Radiat. Isot.* 118 (2016) 124–130, <https://doi.org/10.1016/j.apradiso.2016.09.004>. URL:<https://www.sciencedirect.com/science/article/pii/S0969804316306649>.
- [16] M. Sharifian, M. Sadeghi, B. Alirezapour, Utilization of geant to calculation of production yield for 89zr by charge particles interaction on 89y, natzr and natSr, *Appl. Radiat. Isot.* 127 (2017) 161–165, <https://doi.org/10.1016/j.apradiso.2017.06.005>. URL:<https://www.sciencedirect.com/science/article/pii/S0969804317304232>.
- [17] W. Hauser, H. Feshbach, The inelastic scattering of neutrons, *Phys. Rev.* 87 (1952) 366–373, <https://doi.org/10.1103/PhysRev.87.366>. URL:<https://link.aps.org/doi/10.1103/PhysRev.87.366>.
- [18] J.J. Griffin, Statistical model of intermediate structure, *Phys. Rev. Lett.* 17 (1966) 478–481, <https://doi.org/10.1103/PhysRevLett.17.478>. URL:<https://link.aps.org/doi/10.1103/PhysRevLett.17.478>.
- [19] A. Gilbert, A.G.W. Cameron, A composite nuclear-level density formula with shell corrections, *Can. J. Phys.* 43 (1965) 1446–1496, <https://doi.org/10.1139/p65-139>.
- [20] W. Dilg, W. Mannhart, E. Steichele, P. Arnold, Precision neutron total cross section measurements on gold and cobalt in the 40 ?eV-5 meV range, *Zeitschrift für Physik* 264 (1973) 427–444, <https://doi.org/10.1007/bf01391712>.
- [21] A.V. Ignatyuk, J.L. Weil, S. Raman, S. Kahane, Density of discrete levels in ¹¹⁶Sn, *Phys. Rev. C* 47 (1993) 1504–1513, <https://doi.org/10.1103/PhysRevC.47.1504>. URL:<https://link.aps.org/doi/10.1103/PhysRevC.47.1504>.
- [22] M. Yiğit, A review of (n,p) and (n,α) nuclear cross sections on palladium nuclei using different level density models and empirical formulas, *Appl. Radiat. Isot.* 140 (2018) 355–362, <https://doi.org/10.1016/j.apradiso.2018.08.004>.
- [23] M. Yiğit, A. Kara, Simulation study of the proton-induced reaction cross sections for the production of ¹⁸F and ⁶⁶⁻⁶⁸Ga radioisotopes, *J. Radioanal. Nucl. Chem.* 314 (2017) 2383–2392, <https://doi.org/10.1007/s10967-017-5613-3>.
- [24] M. Yiğit, Analysis of cross sections of (n,t) nuclear reaction using different empirical formulae and level density models, *Appl. Radiat. Isot.* 139 (2018) 151–158, <https://doi.org/10.1016/j.apradiso.2018.05.008>.
- [25] M. Yiğit, Study of cross sections for (n,p) reactions on Hf, Ta and W isotopes, *Appl. Radiat. Isot.* 174 (2021) 109779, <https://doi.org/10.1016/j.apradiso.2021.109779>.
- [26] M. Yiğit, Investigation of (n,2n) reaction cross sections on Pd and Cd isotopes using equilibrium and pre-equilibrium models, *Appl. Radiat. Isot.* 166 (2020) 109399, <https://doi.org/10.1016/j.apradiso.2020.109399>.
- [27] M. Yiğit, Study on (n,p) reactions of ^{58,60,61,62,64}Ni using new developed empirical formulas, *Nucl. Eng. Technol.* 52 (2020) 791–796, <https://doi.org/10.1016/j.net.2019.10.009>.
- [28] M. Yiğit, Theoretical study of cross sections of proton-induced reactions on cobalt, *Nucl. Eng. Technol.* 50 (2018) 411–415, <https://doi.org/10.1016/j.net.2018.01.008>.